Optical Coherence Tomography of Coronary Atherosclerosis

8

Manabu Kashiwagi, Hironori Kitabata,
Takashi Akasaka, and Guillermo J. Tearney

Introduction

Intravascular optical coherence tomography (IVOCT) is an invasive, catheter-based, cross-sectional microscopic imaging technology that employs near-infrared light and provides a depth-dependent resolution of approximately 10 μm and a lateral resolution of about 30 μm [1]. The resolution of IVOCT makes it possible to characterize the detailed structure of the superficial artery wall. IVOCT has been shown to be capable of classifying coronary plaque and various components related to atherosclerosis in vivo, which may provide an improved understanding of atherosclerosis and acute coronary syndrome (ACS) [2–6]. IVOCT may also enable the detection of certain types of "vulnerable plaque" in vivo as well as their clinical features and prognosis [7]. With respect to coronary intervention, IVOCT trials have revealed the association between IVOCT morphological information and adverse cardiac events [8]. It is expected that this improved level of detailed information will help cardiologists make more informed decisions, which will in turn improve patient interventional outcomes. In this chapter, we will provide an introduction to IVOCT imaging, including a brief description of the technology, image interpretation, and areas of further research.

M. Kashiwagi, MD
Wellman Center for Photomedicine, Massachusetts General Hospital, 40 Blossome Street, RSH 160, Boston, MA 02114, USA
e-mail: mkashiwagi2@partners.org

H. Kitabata, MD, PhD • T. Akasaka, MD, PhD
Department of Cardiovascular Medicine, Medical University, 811-1, Kimiidera, Wakayama 641-8509, Japan
e-mail: miu1205@hotmail.co.jp; akasat@wakayama-med.ac.jp

G.J. Tearney, MD, PhD (✉)
Department of Pathology, Massachusetts General Hospital, 40 Parkman Street, RSL 160, Boston, MA 02114, USA
e-mail: gtearney@partners.org

Optical Coherence Tomography

IVOCT is an interferometric imaging technology that uses near-infrared light to obtain information as a function of depth from the luminal surface. IVOCT can provide an axial (depth) resolution of approximately 10 μm and a transverse resolution that ranges between 20 and 40 μm. To obtain optical coherence tomography (OCT) images from vessels such as in the coronary artery, blood needs to be removed from the field of view because near-infrared light is attenuated by the presence of red blood cells. With the first-generation form of IVOCT, termed time-domain OCT (TD-OCT), two methods were used for image acquisition: a balloon occlusion method and a continuous flushing method [6, 9]. However, images were obtained at a slow rate and patients could be exposed to temporary myocardial ischemia to obtain clear images using these flushing methods.

S.J. Nicholls and T. Crowe (eds.), *Imaging Coronary Atherosclerosis*, Contemporary Cardiology,
DOI 10.1007/978-1-4939-0572-0_8,

FD-OCT and OFDI

Frequency domain OCT (FD-OCT) or optical frequency domain imaging (OFDI) is the second-generation form of OCT that is able to acquire images at frame rates that are more than an order magnitude higher than those of TD-OCT [10]. Due to high-speed image acquisition of these technologies, three-dimensional comprehensive volumetric microscopy of long arterial segments can be obtained using an 8–10 cm^3 radiocontrast or saline flush and helically scanning the catheter's optics [11].

Ex Vivo Studies

Normal Vessels

The normal vessel wall is composed of three layers: intima, media, and adventitia. While intravascular ultrasound (IVUS) cannot completely distinguish the boundary of intima and media if the thickness of intima is less than 180 μm [12], IVOCT is capable of detecting intimal thicknesses that are much smaller. In an OCT image, the normal vessel wall is characterized by a layered architecture, comprising a highly backscattering or signal-rich intima, a media that frequently has low backscattering or is signal poor, and heterogeneous and frequently highly backscattering adventitia (Fig. 8.1 and Table 8.1). On occasion, the internal elastic membrane and external elastic membrane are visualized as highly backscattering thin structures that flank the media [7].

Plaque Characterization

Criteria for OCT plaque characterization have been previously established by investigating 357 specimens (162 aortas, 105 carotid bulbs, and 90 coronary arteries) from 90 cadavers [8]. Fibrous plaques were characterized by high scattering and homogeneous signal, fibrocalcific plaque as a signal-poor lesion or heterogeneous region with a

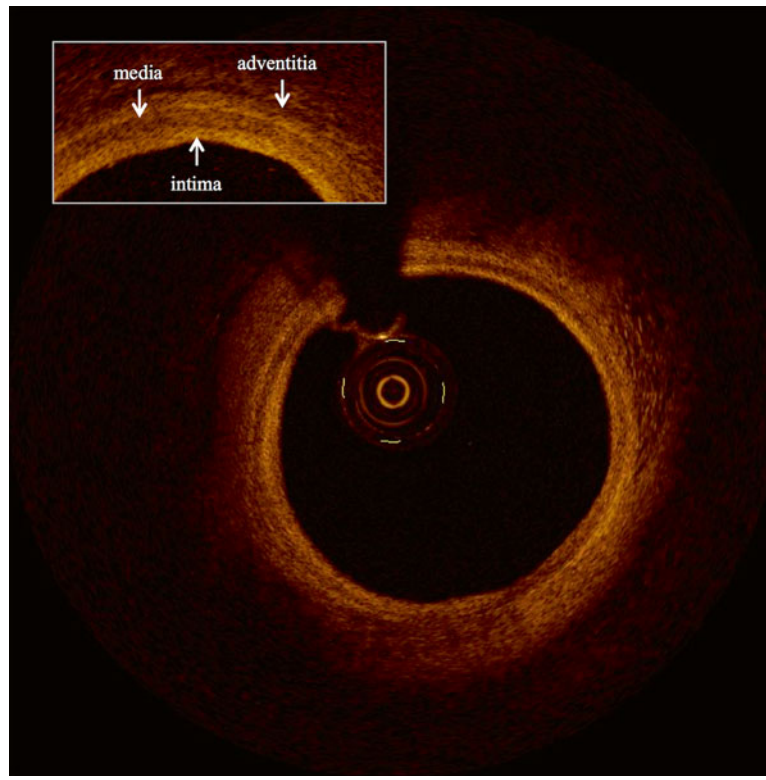

Fig. 8.1 Normal artery wall. Normal artery wall shows a three-layered architecture, comprising a high backscattering, thin intima, a low backscattering media, and a heterogeneous and/or high backscattering adventitia (Courtesy of Wakayama Medical University)

Table 8.1 OCT image features of vessel wall

Histology	OCT
Intima	Signal-rich layer nearest lumen
Media	Signal-poor middle layer
Adventitia	Signal-rich heterogeneous outer lumen
Internal elastic lamina (IEL)	Signal-rich band between intima and media
External elastic lamina (EEL)	Signal-rich band between media and adventitia

Reprinted from Jang IK, Bouma BE, Kang DH, Park SJ, Park SW, Seung KB, et al. Visualization of coronary atherosclerotic plaques in patients using optical coherence tomography: comparison with intravascular ultrasound. J Am Coll Cardiol. 2002;39(4):604–9. With permission from Elsevier

sharply delineated border, and lipid-rich plaques by signal-poor area with diffuse borders (Figs. 8.2 and 8.3). These criteria demonstrated a sensitivity and specificity of 71–79 % and 97–98 % for fibrous plaques, 95–96 % and 97 % for fibrocalcific plaques, and 90–94 % and 90–92 % for lipid-rich plaques, respectively [8]. These results were also confirmed in other ex vivo studies, which showed even higher accuracy of evaluation for lipid-rich plaque compared to IVUS [13].

Macrophages

Macrophages play a key role in all phases of coronary artery atherosclerosis. It has been hypothesized that macrophages show high backscattering because they contain lipid and other cellular debris (Fig. 8.4). In a one study of 27 cadaver necrotic core fibroatheromas, OCT images were acquired and quantified using the "Normalized Standard Deviation" (NSD) parameter that measures local OCT image heterogeneity. NSD was compared to registered histologic slides that were immunohistochemically stained by CD68 [3]. A positive correlation between OCT and histologic measurement of CD68 was found ($r=0.84$, $p<0.00001$); a range of NSD thresholds (6.15–6.35 %) demonstrated 100 % sensitivity and specificity for differentiating caps containing >10 % CD68 staining [3].

Thrombi

OCT can distinguish two major types of thrombi: red and white (Fig. 8.5). The red thrombus shows high backscattering and high attenuation. In contrast, the white thrombus shows less backscattering, low attenuation, and a homogeneous signal [4]. The appearance of mixed and organized thrombi by OCT is hypothesized to be heterogeneous, but the image characteristics of organized thrombi are not well understood or validated.

Cholesterol Crystals

Cholesterol crystals can be seen by IVOCT within atheromatous plaque, usually in combination with lipid. Cholesterol crystals appear as needle-shaped clefts on pathology and OCT demonstrates similarly shaped, linear highly scattering signals [5] (Fig. 8.6). Some investigators have suggested that cholesterol crystal might have the potential to injure the fibrous cap, leading to ACS, but to date, there are no in vivo OCT examinations or trials that test this hypothesis [14].

Neovascularization

Vulnerable plaque is pathologically defined as a plaque with a thin fibrous cap, necrotic core, and macrophage infiltration within a fibrous cap. In addition, neovascularization in atheromatous plaque, called "vasa vasorum," may also be related to plaque vulnerability [15]. Neovascularization is identified as regions with little or no IVOCT backscattering and are frequently observed over several frames [16] (Fig. 8.7). Although there is little histopathologic validation of IVOCT for neovascularization, a clinical OCT study demonstrates that these regions in coronary plaques correlate with the presence of thin-cap fibroatheromas (TCFA) and positive arterial remodeling [17]. More recently, it has been reported that neovascularization seen by IVOCT is strongly associated with the progression of coronary artery plaques [18].

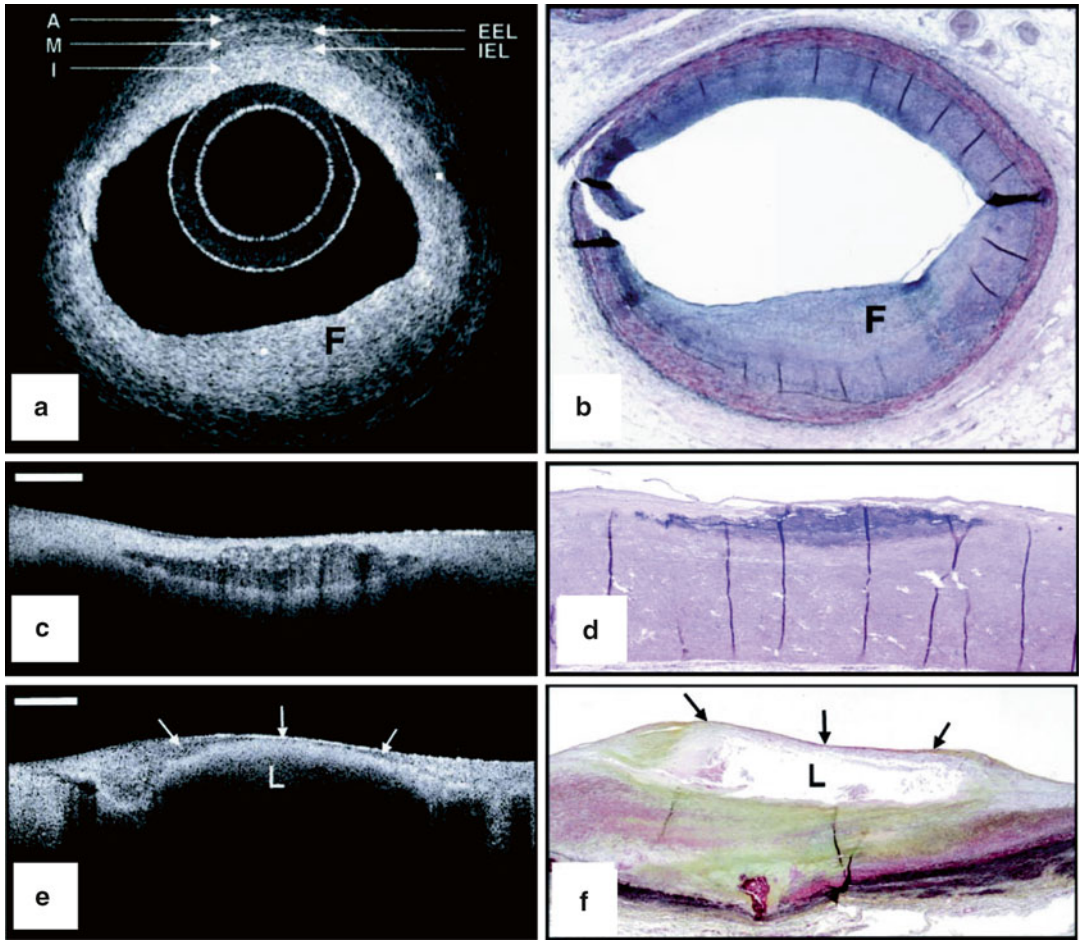

Fig. 8.2 Ex vivo OCT images of human plaques. (**a**) OCT image of a fibrous coronary plaque showing a homogeneous, signal-rich interior (F). An area of intimal hyperplasia is seen opposite fibrous lesion, demonstrating intima (I, with intimal hyperplasia), internal elastic lamina (IEL), media (M), external elastic lamina (EEL), and adventitia (A). (**b**) Corresponding histology (Movat's pentachrome; magnification ×40). (**c**) OCT image of a fibrocalcific aortic plaque showing a sharply delineated region with a signal-poor interior. Bar = 500 μm. (**d**) Corresponding histology (H&E; magnification ×40). (**e**) OCT image of a lipid-rich carotid plaque showing a signal-poor lipid pool (L) with poorly delineated borders beneath a thin homogeneous band, corresponding to fibrous cap (*arrows*). Bar = 500 μm. (**f**) Corresponding histology (Movat's pentachrome; magnification ×20) (Reprinted from Yabushita H, Bouma BE, Houser SL, Aretz HT, Jang IK, Schlendorf KH, et al. Characterization of human atherosclerosis by optical coherence tomography. Circulation. 2002;106(13):1640–5. With permission from Wolters Kluwer Health)

Fig. 8.4 Ex vivo OCT image of macrophages. Raw (**a**) and logarithm base 10 (**b**) OCT images of a fibroatheroma with a low density of macrophages within the fibrous cap. (**c**) Corresponding histology for (**a**) and (**b**) (CD68 immunoperoxidase; original magnification ×100). Raw (**d**) and logarithm base 10 (**e**) OCT images of a fibroatheroma with a high density of macrophages within the fibrous cap. (**f**) Corresponding histology for (**d**) and (**e**) (CD68 immunoperoxidase; original magnification ×100) (Reprinted from Tearney GJ, Yabushita H, Houser SL, Aretz HT, Jang IK, Schlendorf KH, Kauffman CR, Shishkov M, Halpern EF, Bouma BE. Quantification of macrophage content in atherosclerotic plaques by optical coherence tomography. Circulation. 2003;107(1):113–9. With permission from Wolters Kluwer Health)

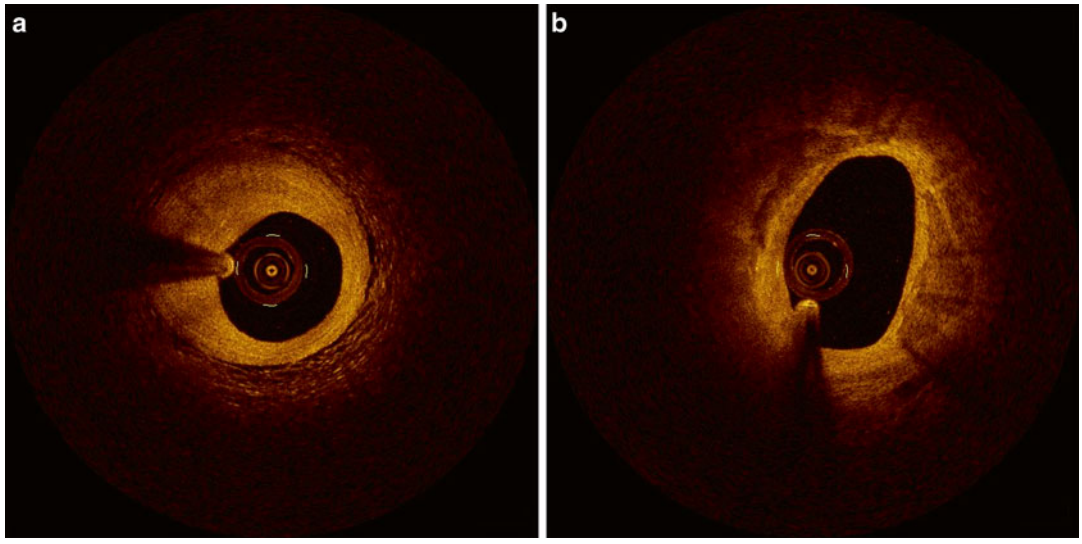

Fig. 8.3 In vivo coronary artery plaques. (**a**) Fibrous plaque. High scattering and homogeneous signal is observed. (**b**) Fibrocalcified plaque. Signal-poor heterogeneous region on both sides with well-delineated borders (Courtesy of Wakayama Medical University)

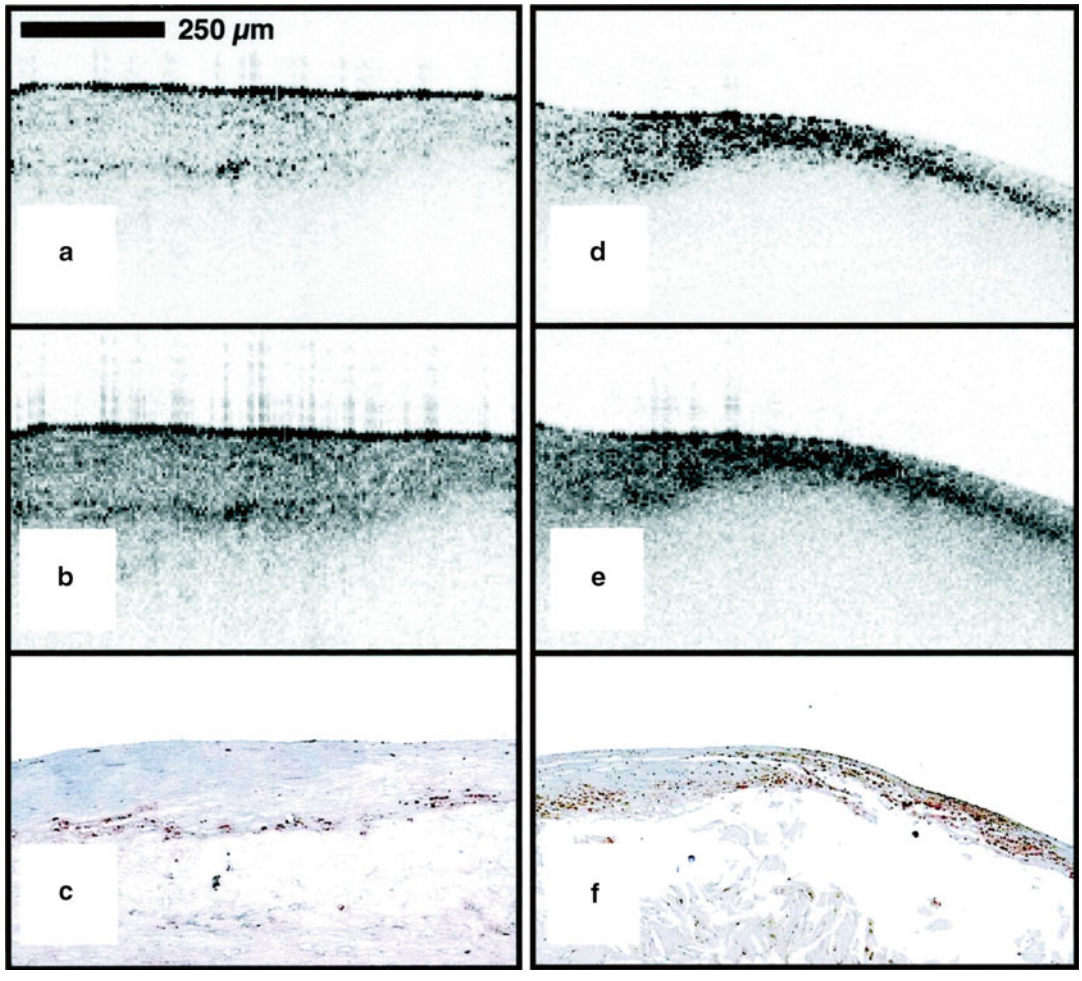

Fig. 8.4 (continued)

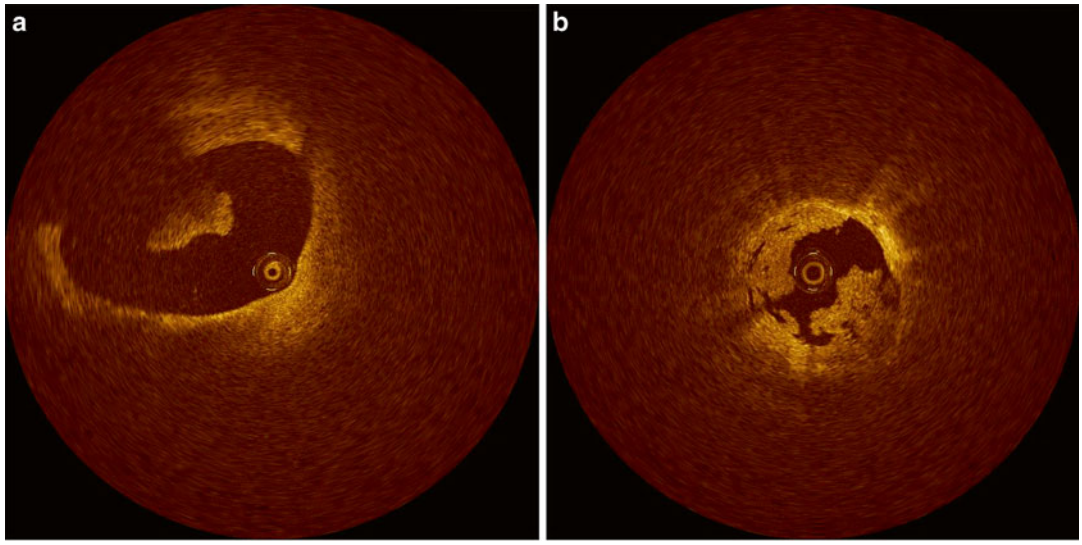

Fig. 8.5 Thrombi. (**a**) Red thrombus. A red thrombus with high IVOCT backscattering and attenuation is floating in the coronary artery. (**b**) White thrombus. White thrombus with homogeneous backscattering and low attenuation attached to coronary artery wall (Courtesy of Wakayama Medical University)

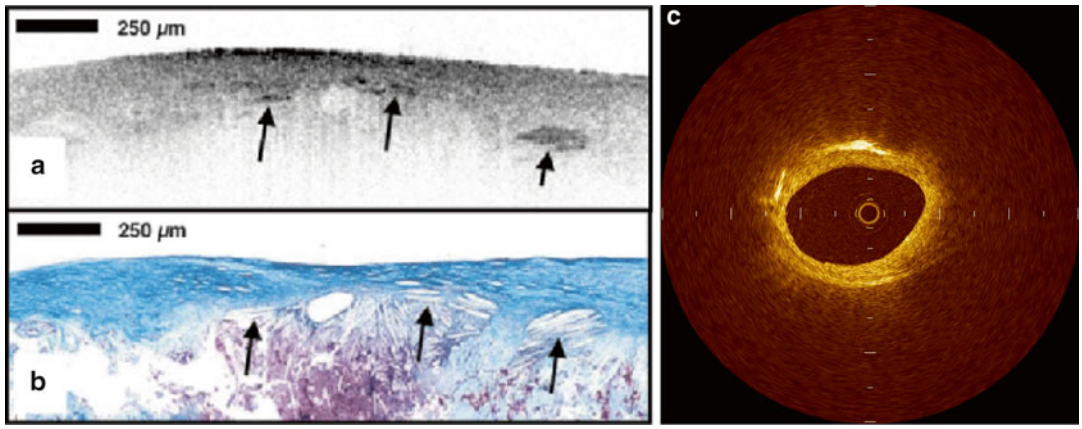

Fig. 8.6 Cholesterol crystal. OCT image (**a**) demonstrates oriented, linear, highly reflecting structures near the fibrous cap-lipid pool junction (*arrows*). Corresponding histology (**b**, Masson's trichrome; original magnification ×40) demonstrated the presence of cholesterol crystals (*arrows*). Cholesterol crystals in vivo OCT image (**c**) appears as linear, highly backscattering structures within in the plaque (Reprinted from Tearney GJ, Jang IK, Bouma BE. Evidence of Cholesterol Crystals in Atherosclerotic Plaque by Optical Coherence Tomographic (OCT) Imaging. Eur. Heart J. 2003:23;1462. With permission from Oxford University Press)

In Vivo Studies

Detection of Vulnerable Plaques

For cardiologists, the detection of vulnerable plaques, the most common of which is the TCFA, is a key goal for predicting and preventing the course of ACS. On IVOCT assessment, TCFA has been defined by some as a plaque with ≥2 quadrants of lipid and the thinnest part of a fibrous cap measuring <65 μm. In one study, 57 patients who underwent successful percutaneous coronary intervention (PCI) were divided into three groups: acute myocardial infarction (AMI) ($n = 20$), ACS ($n = 20$), and stable angina pectoris (SAP) ($n = 17$). Patients with AMI and ACS demonstrated higher incidence of TCFA

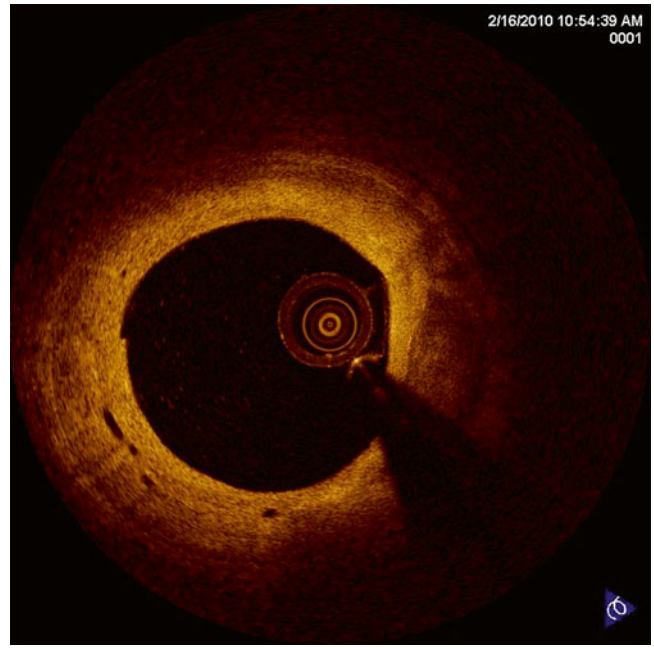

Fig. 8.7 Neovascularization. Intimal vessels are well-delineated regions or voids with low OCT backscattering (Courtesy of Wakayama Medical University)

and thinner fibrous cap thickness compared with SAP [19].

Frequency and distribution of TCFA were also examined, and pathology reports that indicated TCFA defined by OCT were dominant in the proximal left anterior descending artery, whereas TCFA in the left circumflex artery and the right coronary artery were equally distributed [20, 21]. As with culprit lesions, TCFA in non-culprit lesions were more frequent in patients with ACS than SAP [22].

The alternative criteria of TCFA recently have been proposed by OCT consensus document [23]. An OCT-TCFA is defined as an IVOCT-delineated necrotic core with an overlying fibrous cap in which the minimum thickness of the fibrous cap is less than a predetermined threshold. The clinical significance of lipid arc dimensions was determined to be unknown and remains an area of future investigation [23].

Macrophages In Vivo

Macrophage content was investigated in vivo in a study that enrolled 49 patients undergoing PCI [24] where again patients were divided into three groups: ST-elevation myocardial infarction (STEMI) ($n = 19$), ACS ($n = 19$), and SAP ($n = 11$). Macrophages were measured in the caps of IVOCT-determined fibroatheroma. NSD values showed a relationship between macrophage concentrations and the various clinical presentations. Patients with unstable clinical presentation had higher concentrations of macrophages and macrophage densities correlated with white blood count, the thickness of the fibrous cap, and arterial remodeling [25, 26]. Further, macrophage density was found to be higher at cap rupture sites of culprit lesions than at non-rupture sites (Fig. 8.8). Even though these results have showed interesting relationships between macrophages and other clinical and microstructural findings, the clinical implication of NSD measurements by OCT, especially prognostic value, remains unknown.

Acute Coronary Syndrome

New findings from clinical studies have elucidated some of the intricacies of ACS [27–30]. For example, IVOCT demonstrated that the morphologies of exertion-triggered and rest-onset ruptured plaques differ in ACS patients,

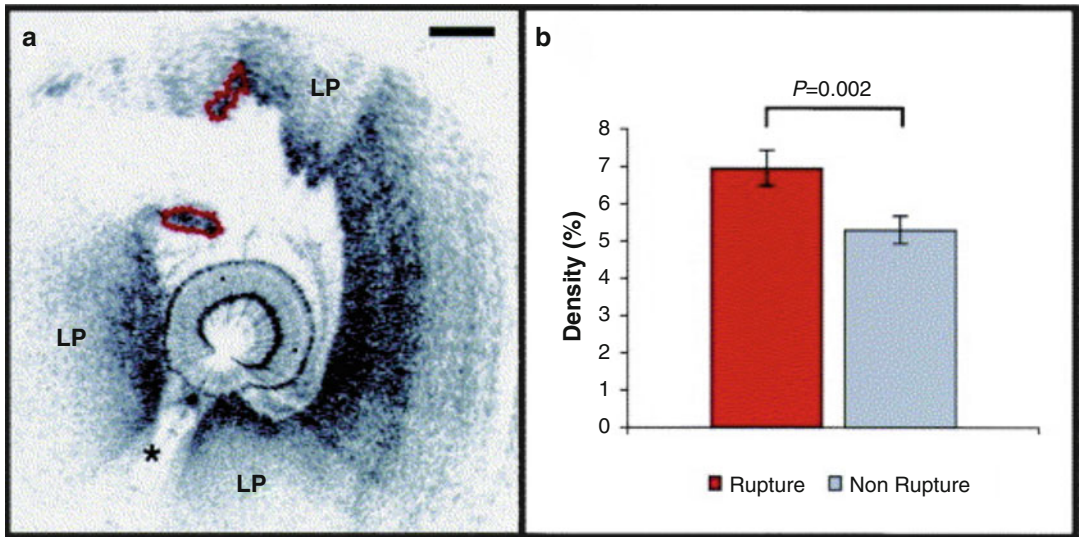

Fig. 8.8 Intracoronary OCT macrophage imaging. (**a**) Optical coherence tomography (OCT) image of a rupture site (outlined in *red*) overlying a lipid-rich plaque (LP). The *asterisk* symbol represents guide wire shadow. A 500 **μ**m scale bar is seen in the *top right-hand corner*. (**b**) Bar graph representing mean macrophage density at sites of rupture, corresponding to outlined segment in panel (**a**), compared with the rest of the plaque. Standard error bars are represented. (Reprinted from MacNeill BD, Jang IK, Bouma BE, Iftimia N, Takano M, Yabushita H, et al. Focal and multifocal plaque macrophage distributions in patients with acute and stable presentations of coronary artery disease. J Am Coll Cardiol. 2004;44(5):972–9. With permission from Elsevier)

and that some plaque ruptures may occur in thick fibrous caps, up to 140 μm, depending on exertion levels [27] (Fig. 8.9). Another IVOCT trial reported the differences in culprit lesion morphology between STEMI and non-ST-segment elevation acute coronary syndrome (NSTEACS). As a result, culprit lesions in STEMI showed higher incidence of plaque rupture, TCFA, and red thrombus than those in NSTEACS [28]. Patients with STEMI also had greater plaque disruption and smaller minimal lumen area than patients with NSTEM [29]. These results suggest that the indicate that morphological features at culprit lesions could relate to the clinical presentation in patients with acute coronary disease. Moreover, IVOCT revealed a relationship between lesion morphology on OCT and Braunwald classification of unstable angina pectoris (UAP). Patients with class II UAP more frequently showed plaque rupture and thrombosis formation [30]. These findings suggest that IVOCT may provide a novel means for exploring the pathophysiology of ACS in vivo.

Prognosis

IVOCT has also revealed findings regarding the natural history of coronary artery disease. In one recent clinical study, the percent changes in fibrous cap thickness assessed by OCT correlated with the percent changes in external elastic membrane cross-sectional area within a time frame of 6 months [31]. In another study, the change in high-sensitivity C-reactive protein was also found to be significantly correlated with changes in fibrous cap thickness [32]. OCT studies have revealed certain aspects about the effects of medical therapy on the coronary artery. Statin therapies have been found to be related to increased fibrous cap thickness, reduced plaque volume, and overall a more stable coronary structural phenotype [33, 34]. One IVOCT trial revealed that TCFA and neovascularization are independent predictors of luminal progression [18]. These results support the notion that TCFA leads to plaque progression in vivo. Nevertheless, the question of whether or not

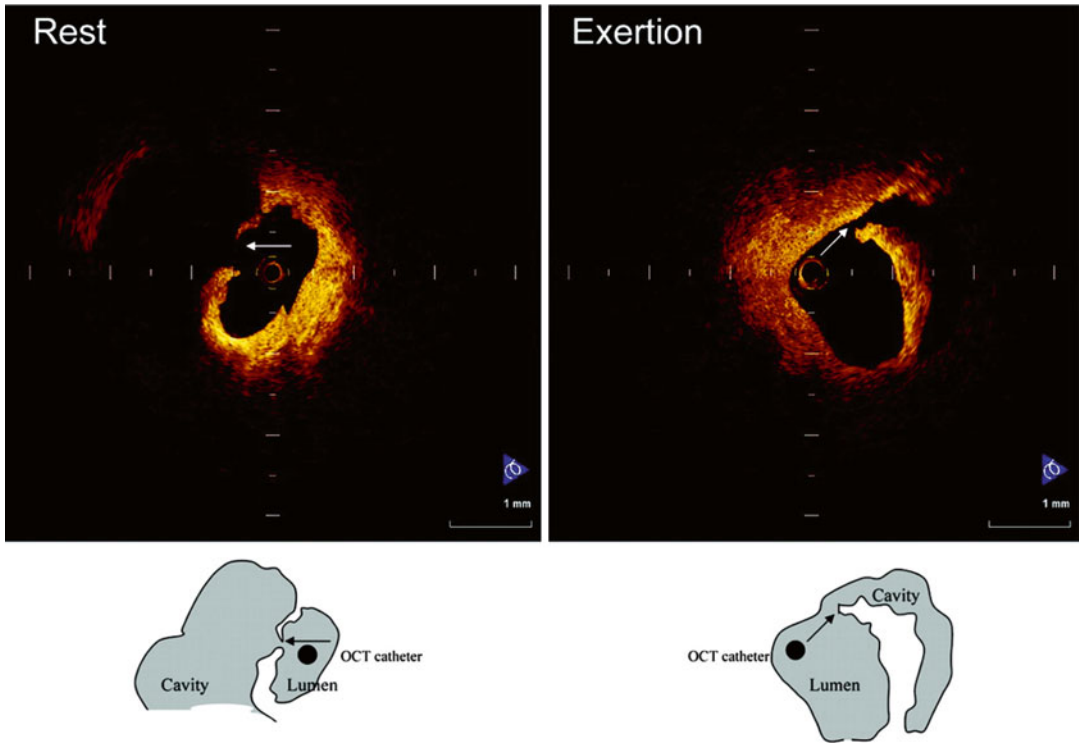

Fig. 8.9 Representative cases of plaque rupture occurring at rest or with exertion. (*Left*) Plaque rupture that occurred at rest. Fibrous cap was broken at the midportion, and a thin fibrous cap could be observed. (*Right*) Plaque rupture that occurred during heavy farm work. Thick fibrous cap was broken at shoulder of plaque (Reprinted from Tanaka A, Imanishi T, Kitabata H, Kubo T, Takarada S, Tanimoto T, et al. Morphology of exertion-triggered plaque rupture in patients with acute coronary syndrome: an optical coherence tomography study. Circulation. 2008;118:2368–73. With permission from Wolters Kluwer Health)

OCT-derived TCFA leads to ACS in real-world scenarios still remains.

Neoatherosclerosis in Stented Lesions

A recent pathological study showed that neoatherosclerosis and consequent plaque vulnerability can occur in previously stented lesions 5 years after bare-metal stent (BMS) placement [35]. An in vivo OCT observational study revealed that late-phase BMS (>5 years) showed higher incidence of vulnerable atherosclerotic changes, including lipid-laden intima, intimal disruption, and thrombus, than early-phase BMS (<6 months) [36]. In some cases, neoatherosclerosis in BMS eventually led to plaque rupture and secondary thrombus formation, resulting in ACS [37] (Fig. 8.10). Also in drug-eluting stents (DES), neoatherosclerosis is a frequent finding and pathologically can occur earlier than in BMS, potentially due to more pronounced inflammation related to drug and durable polymer [38]. In vivo OCT examination revealed that late-phase DES (>20 months) had a higher incidence of TCFA-containing neointima and red thrombus [39]. Even though DES has been reported to greatly reduce restenosis and offer an effective approach to coronary artery disease, 0.4–0.6 % annual incidences of late stent thrombosis (LST) occurs rarely. Neoatherosclerosis and subsequent plaque rupture in DES are considered to be one of the potential causes of LST [40].

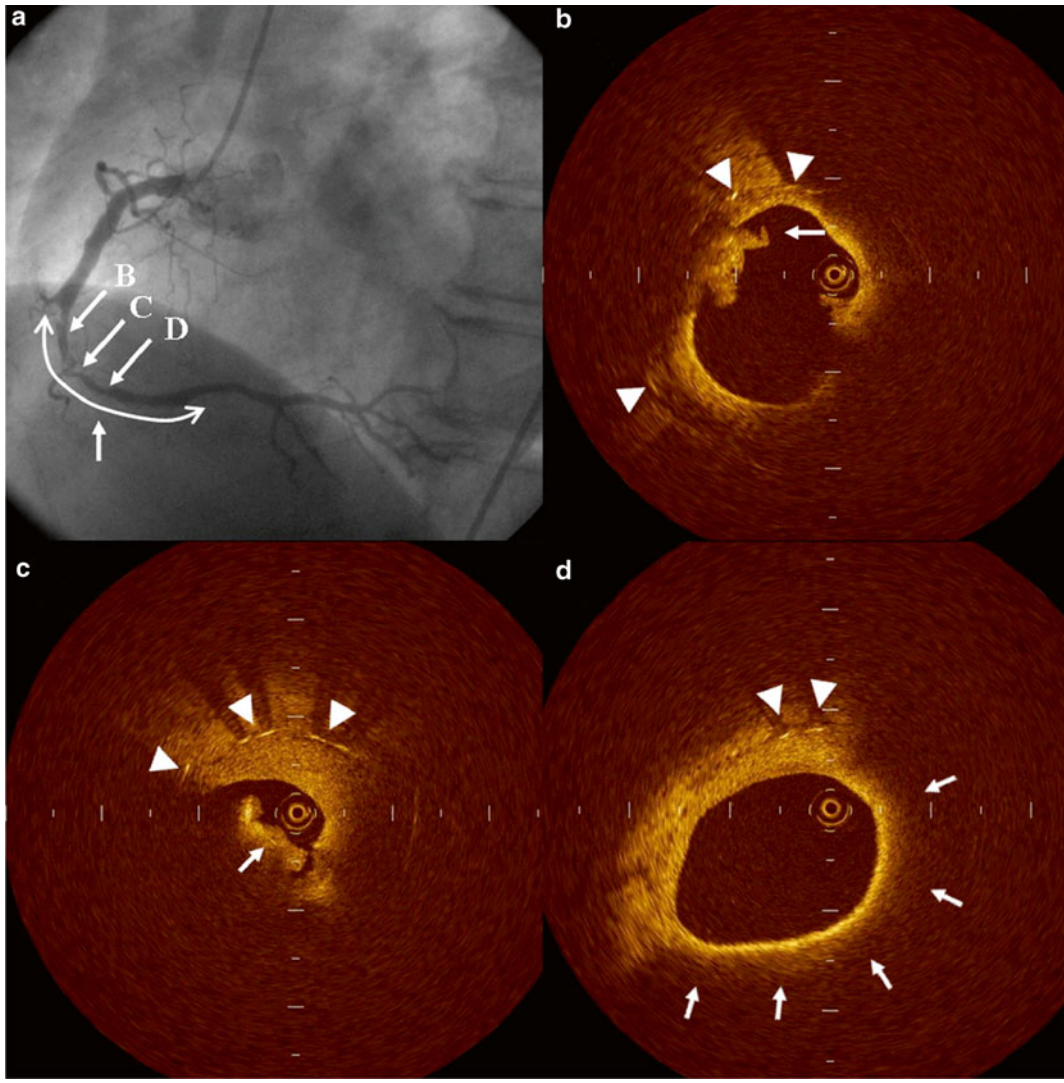

Fig. 8.10 Neoatherosclerosis and acute event at late phase BMS. An emergent coronary angiogram showed severe in-stent stenosis in the previously stented segment (**a**). OCT examination demonstrated plaque rupture in the stented segment (**b**). The thickness of broken fibrous cap was 40 μm. Intracoronary thrombus was also visualized as a mass protruding into the vessel lumen (**c**). Lipid-rich plaque (*arrow*) covered by thin fibrous cap (60 μm) was imaged and determined as a thin-cap fibroatheroma (**d**). *Arrow head* indicates stent strut (Reprinted from Kashiwagi M, Kitabata H, Tanaka A, Okochi K, Ishibashi K, Komukai K, et al. Very late clinical cardiac event after BMS implantation: in vivo optical coherence tomography examination. JACC Cardiovasc Imaging. 2010;3(5):525–7. With permission from Elsevier)

Percutaneous Coronary Intervention

Like IVUS-guided PCI, IVOCT-guided intervention is still a concept under investigation [41–46]. IVOCT-derived lipid plaque is considered as a predictor for no-reflow phenomenon and post-PCI creatine kinase elevation [8, 47]. Moreover, as compared to IVUS, OCT can potentially more accurately detect adverse events after stenting, including stent-edge dissection, tissue protrusion, and malapposition [48]. Regarding OCT-guided intervention, Imola et al. conducted a single-center registry to evaluate the safety and feasibility of OCT-guided PCI and they con-

cluded FD-OCT has potential to become a safety guidance tool for PCI [49]. In another retrospective trial, IVOCT demonstrated adverse features requiring further intervention in 34.7 % patients and OCT-guided intervention provided a significantly lower risk of cardiac death or myocardial infarction event compared to angiography-guided intervention [50]. However, because evidence about OCT-guided intervention is not fully elucidated, this issue needs to be investigated in further outcome-based studies that reveal which information extracted from IVOCT images can be used during intervention to improve patient outcome.

Future Developments

A newer OCT technology, termed "micro OCT" (μOCT), has ten times greater resolution (approximately 1 μm) than conventional IVOCT [51]. The higher resolution of μOCT makes it possible to image cellular and subcellular morphologic features associated with atherogenesis, thrombosis, and responses to interventional therapy. In the first study to demonstrate this technology ex vivo, macrophage foam cells and cholesterol crystals were clearly visualized. μOCT also enabled the detection of DES polymer in cadaver specimens, which is difficult to appreciate in currently available IVOCT systems. Another technological advancement is the combination of IVOCT with other imaging technologies. Recently, a dual-modality, catheter-based combination of IVOCT and near-infrared fluorescence (NIRF) imaging [52] has been shown and demonstrated in rabbits in vivo. This multimodality technology simultaneously provides images of colocalized molecular and microstructural information [52]. This technology has the potential to enable the detection of fibrin over stents, which could in the future be used to inform decisions regarding antiplatelet therapy [52]. It furthermore can assess enzymatic activity in the context of the microstructure of the plaque [52]. The unique capabilities of NIRF-OFDI may make it a valuable tool for assessing atherosclerosis and stent healing at both the molecular and microstructural levels.

Conclusion

IVOCT has been demonstrated to clearly enable the visualization of microstructural features of the superficial coronary wall. The advent of second-generation forms of IVOCT has made it practical to use this technology in the cardiovascular catheterization lab. While this technology is very promising for investigating plaque structure, composition, and the stent healing process, much needs to be learned regarding its ability to be used to guide intervention and improve patient outcomes. Future generation IVOCT technologies offer the promise of imaging cells and subcellular structures in the coronary wall and simultaneously obtaining molecular and microstructural information. The promise of today's IVOCT and future iterations of this technology makes this field a very interesting area for research and clinical application development.

Acknowledgements We gratefully acknowledge Takashi Akasaka, MD and Hironori Kitabata, MD for providing clinical in vivo OCT images.

Disclosure: Massachusetts General Hospital has a licensing arrangement with Terumo Corporation regarding IVOCT technology. Dr. Tearney has the right to receive royalties as part of this licensing arrangement. Dr. Tearney receives sponsored research from Canon Corporation.

References

1. Bouma BE, Tearney GJ. Power-efficient nonreciprocal interferometer and linear-scanning fiber-optic catheter for optical coherence tomography. Opt Lett. 1999;24(8):531–3.
2. Yabushita H, Bouma BE, Houser SL, Aretz HT, Jang IK, Schlendorf KH, et al. Characterization of human atherosclerosis by optical coherence tomography. Circulation. 2002;106(13):1640–5.
3. Tearney GJ, Yabushita H, Houser SL, Aretz HT, Jang IK, Schlendorf KH, et al. Quantification of macrophage content in atherosclerotic plaques by optical coherence tomography. Circulation. 2003;107(1):113–9.
4. Kume T, Akasaka T, Kawamoto T, Ogasawara Y, Watanabe N, Toyota E, et al. Assessment of coronary arterial thrombus by optical coherence tomography. Am J Cardiol. 2006;97(12):1713–7.
5. Tearney GJ, Jang IK, Bouma BE. Evidence of cholesterol crystals in atherosclerotic plaque by optical coherence tomographic (OCT) imaging. Eur Heart J. 2003;23:1462.

6. Prati F, Regar E, Mintz GS, Arbustini E, Di Mario C, Jang IK, et al. Expert review document on methodology, terminology, and clinical applications of optical coherence tomography: physical principles, methodology of image acquisition, and clinical application for assessment of coronary arteries and atherosclerosis. Eur Heart J. 2010;31:401–15.
7. Jang IK, Bouma BE, Kang DH, Park SJ, Park SW, Seung KB, et al. Visualization of coronary atherosclerotic plaques in patients using optical coherence tomography: comparison with intravascular ultrasound. J Am Coll Cardiol. 2002;39(4):604–9.
8. Tanaka A, Imanishi T, Kitabata H, Kubo T, Takarada S, Tanimoto T, et al. Lipid-rich plaque and myocardial perfusion after successful stenting in patients with non-ST-segment elevation acute coronary syndrome: an optical coherence tomography study. Eur Heart J. 2009;30:1348–55.
9. Kataiwa H, Tanaka A, Kitabata H, Matsumoto H, Kashiwagi M, Kuroi A, et al. Head to head comparison between the conventional balloon occlusion method and the non-occlusion method for optical coherence tomography. Int J Cardiol. 2011;146(2): 186–90.
10. Yun SH, Tearney GJ, Vakoc BJ, Shishkov M, Oh WY, Desjardins AE, et al. Comprehensive volumetric optical microscopy in vivo. Nat Med. 2006;12(12): 1429–33.
11. Tearney GJ, Waxman S, Shishkov M, Vakoc BJ, Suter MJ, Freilich MI, et al. Three-dimensional coronary artery microscopy by intracoronary optical frequency domain imaging. JACC Cardiovasc Imaging. 2008; 1(6):752–61.
12. Fitzgerald PJ, St Goar FG, Connolly AJ, Pinto FJ, Billingham ME, Popp RL, et al. Intravascular ultrasound imaging of coronary arteries. Is three layers the norm? Circulation. 1992;86(1):154–8.
13. Kume T, Akasaka T, Kawamoto T, Watanabe N, Toyota E, Neishi Y, et al. Assessment of coronary arterial plaque by optical coherence tomography. Am J Cardiol. 2006;97(8):1172–5.
14. Abela GS, Aziz K, Vedre A, Pathak DR, Talbott JD, Dejong J. Effect of cholesterol crystals on plaques and intima in arteries of patients with acute coronary and cerebrovascular syndromes. Am J Cardiol. 2009; 103(7):959–68.
15. Moreno PR, Purushothaman KR, Fuster V, Echeverri D, Truszczynska H, Sharma SK, et al. Plaque neovascularization is increased in ruptured atherosclerotic lesions of human aorta: implications for plaque vulnerability. Circulation. 2004;110:2032–8.
16. Vorpahl M, Nakano M, Virmani R. Small black holes in optical frequency domain imaging matches intravascular neoangiogenesis formation in histology. Eur Heart J. 2010;31(15):1889.
17. Kitabata H, Tanaka A, Kubo T, Takarada S, Kashiwagi M, Tsujioka H, et al. Relation of microchannel structure identified by optical coherence tomography to plaque vulnerability in patients with coronary artery disease. Am J Cardiol. 2010;105(12):1673–8.
18. Uemura S, Ishigami K, Soeda T, Okayama S, Sung JH, Nakagawa H, et al. Thin-cap fibroatheroma and microchannel findings in optical coherence tomography correlate with subsequent progression of coronary atheromatous plaques. Eur Heart J. 2012; 33(1):78–85.
19. Jang IK, Tearney GJ, MacNeill B, Takano M, Moselewski F, Iftima N, et al. In vivo characterization of coronary atherosclerotic plaque by use of optical coherence tomography. Circulation. 2005;111(12): 1551–5.
20. Tanaka A, Imanishi T, Kitabata H, Kubo T, Takarada S, Kataiwa H, et al. Distribution and frequency of thin-capped fibroatheromas and ruptured plaques in the entire culprit coronary artery in patients with acute coronary syndrome as determined by optical coherence tomography. Am J Cardiol. 2008;102(8):975–9.
21. Fujii K, Kawasaki D, Masutani M, Okumura T, Akagami T, Sakoda T, et al. OCT assessment of thin-cap fibroatheroma distribution in native coronary arteries. JACC Cardiovasc Imaging. 2010;3(2): 168–75.
22. Kubo T, Imanishi T, Kashiwagi M, Ikejima H, Tsujioka H, Kuroi A, et al. Multiple coronary lesion instability in patients with acute myocardial infarction as determined by optical coherence tomography. Am J Cardiol. 2010;105(3):318–22.
23. MacNeill BD, Jang IK, Bouma BE, Iftimia N, Takano M, Yabushita H, et al. Focal and multi-focal plaque macrophage distributions in patients with acute and stable presentations of coronary artery disease. J Am Coll Cardiol. 2004;44(5):972–9.
24. Tearney GJ, Regar E, Akasaka T, Adriaenssens T, Barlis P, Bezerra HG, et al. Consensus standards for acquisition, measurement, and reporting of intravascular optical coherence tomography studies: a report from the International Working Group for Intravascular Optical Coherence Tomography Standardization and Validation. J Am Coll Cardiol. 2012;59:1058–72.
25. Raffel OC, Tearney GJ, Gauthier DD, Halpern EF, Bouma BE, Jang IK. Relationship between a systemic inflammatory marker, plaque inflammation, and plaque characteristics determined by intravascular optical coherence tomography. Arterioscler Thromb Vasc Biol. 2007;27(8):1820–7.
26. Raffel OC, Merchant FM, Tearney GJ, Chia S, Gauthier DD, Pomerantsev E, et al. In vivo association between positive coronary artery remodelling and coronary plaque characteristics assessed by intravascular optical coherence tomography. Eur Heart J. 2008;29(14):1721–8.
27. Tanaka A, Imanishi T, Kitabata H, Kubo T, Takarada S, Tanimoto T, et al. Morphology of exertion-triggered plaque rupture in patients with acute coronary syndrome: an optical coherence tomography study. Circulation. 2008;118:2368–73.

28. Ino Y, Kubo T, Tanaka A, Kuroi A, Tsujioka H, Ikejima H, et al. Difference of culprit lesion morphologies between ST-segment elevation myocardial infarction and non-ST-segment elevation acute coronary syndrome: an optical coherence tomography study. JACC Cardiovasc Interv. 2011;4(1):76–82.
29. Toutouzas K, Karanasos A, Tsiamis E, Riga M, Drakopoulou M, Synetos A, et al. New insights by optical coherence tomography into the differences and similarities of culprit ruptured plaque morphology in non-ST-elevation myocardial infarction and ST-elevation myocardial infarction. Am Heart J. 2011;161(6):1192–9.
30. Mizukoshi M, Imanishi T, Tanaka A, Kubo T, Liu Y, Takarada S, et al. Clinical classification and plaque morphology determined by optical coherence tomography in unstable angina pectoris. Am J Cardiol. 2010;106(3):323–8.
31. Yamada R, Okura H, Kume T, Saito K, Miyamoto Y, Imai K, et al. Relationship between arterial and fibrous cap remodeling: a serial three-vessel intravascular ultrasound and optical coherence tomography study. Circ Cardiovasc Interv. 2010;3(5):484–90.
32. Takarada S, Imanishi T, Ishibashi K, Tanimoto T, Komukai K, Ino Y, et al. The effect of lipid and inflammatory profiles on the morphological changes of lipid-rich plaques in patients with non-ST-segment elevated acute coronary syndrome: follow-up study by optical coherence tomography and intravascular ultrasound. JACC Cardiovasc Interv. 2010;3(7): 766–72.
33. Hattori K, Ozaki Y, Ismail TF, Okumura M, Naruse H, Kan S, et al. Impact of statin therapy on plaque characteristics as assessed by serial OCT, grayscale and integrated backscatter-IVUS. JACC Cardiovasc Imaging. 2012;5(2):169–77.
34. Takarada S, Imanishi T, Kubo T, Tanimoto T, Kitabata H, Nakamura N, et al. Effect of statin therapy on coronary fibrous-cap thickness in patients with acute coronary syndrome: assessment by optical coherence tomography study. Atherosclerosis. 2009;202(2): 491–7.
35. Inoue K, Abe K, Ando K, Shirai S, Nishiyama K, Nakanishi M, et al. Pathological analyses of long-term intracoronary Palmaz-Schatz stenting; Is its efficacy permanent? Cardiovasc Pathol. 2004;13:109–15.
36. Takano M, Yamamoto M, Inami S, Murakami D, Ohba T, Seino Y, et al. Appearance of lipid-laden intima and neovascularization after implantation of bare-metal stents extended late-phase observation by intracoronary optical coherence tomography. J Am Coll Cardiol. 2009;55(1):26–32.
37. Kashiwagi M, Kitabata H, Tanaka A, Okochi K, Ishibashi K, Komukai K, et al. Very late clinical cardiac event after BMS implantation: in vivo optical coherence tomography examination. JACC Cardiovasc Imaging. 2010;3(5):525–7.
38. Nakazawa G, Otsuka F, Nakano M, Vorpahl M, Yazdani SK, Ladich E, et al. The pathology of neoatherosclerosis in human coronary implants bare-metal and drug-eluting stents. J Am Coll Cardiol. 2011; 57(11):1314–22.
39. Kang SJ, Mintz GS, Akasaka T, Park DW, Lee JY, Kim WJ, et al. Optical coherence tomographic analysis of in-stent neoatherosclerosis after drug-eluting stent implantation. Circulation. 2011;123(25):2954–63.
40. Guagliumi G, Sirbu V, Musumeci G, Gerber R, Biondi-Zoccai G, Ikejima H, et al. Examination of the in vivo mechanisms of late drug-eluting stent thrombosis: findings from optical coherence tomography and intravascular ultrasound imaging. JACC Cardiovasc Interv. 2012;5(1):12–20.
41. Schiele F, Meneveau N, Vuillemenot A, Zhang DD, Gupta S, Mercier M, et al. Impact of intravascular ultrasound guidance in stent deployment on 6-month restenosis rate: a multicenter, randomized study comparing two strategies–with and without intravascular ultrasound guidance. RESIST Study Group. REStenosis after Ivus guided STenting. J Am Coll Cardiol. 1998;32:320–8.
42. Fitzgerald PJ, Oshima A, Hayase M, Metz JA, Bailey SR, Baim DS, et al. Final results of the Can Routine Ultrasound Influence Stent Expansion (CRUISE) study. Circulation. 2000;120:523–30.
43. Mudra H, di Mario C, de Jaegere P, Figulla HR, Macaya C, Zahn R, et al. Randomized comparison of coronary stent implantation under ultrasound or angiographic guidance to reduce stent restenosis (OPTICUS study). Circulation. 2001;104:1343–9.
44. Russo RJ, Silva PD, Teirstein PS, Attubato MJ, Davidson CJ, DeFranco AC, et al. A randomized controlled trial of angiography versus intravascular ultrasound-directed bare-metal coronary stent placement (The AVID Trial). Circ Cardiovasc Interv. 2009;2:113–23.
45. Roy P, Steinberg DH, Sushinsky SJ, Okabe T, Pinto Slottow TL, Kaneshige K, et al. The potential clinical utility of intravascular ultrasound guidance in patients undergoing percutaneous coronary intervention with drug-eluting stents. Eur Heart J. 2008;29:1851–7.
46. Claessen BE, Mehran R, Mintz GS, Weisz G, Leon MB, Dogan O, et al. Impact of intravascular ultrasound imaging on early and late clinical outcomes following percutaneous coronary intervention with drug-eluting stents. J Am Coll Cardiol Intv. 2011; 4:974–81.
47. Yonetsu T, Kakuta T, Lee T, Takahashi K, Yamamoto G, Iesaka Y, et al. Impact of plaque morphology on creatine kinase-MB elevation in patients with elective stent implantation. Int J Cardiol. 2011;146:180–5.
48. Kubo T, Imanishi T, Kitabata H, Kuroi A, Ueno S, Yamano T, et al. Comparison of vascular response after sirolimus-eluting stent implantation between unstable angina pectoris and stable angina pectoris: a serial optical coherence tomography study. J Am Coll Cardiol Img. 2008;1:475–84.
49. Imola F, Mallus MT, Ramazzotti V, Manzoli A, Pappalardo A, Di Giorgio A, et al. Safety and feasibil-

ity of frequency domain optical coherence tomography to guide decision making in percutaneous coronary intervention. EuroIntervention. 2010;6:575–81.
50. Prati F, Di Vito L, Biondi-Zoccai G, Occhipinti M, La Manna A, Tamburino C, et al. Angiography alone versus angiography plus optical coherence tomography to guide decision-making during percutaneous coronary intervention: the Centro per la Lotta contro l'Infarto-Optimisation of Percutaneous Coronary Intervention (CLI-OPCI) study. EuroIntervention. 2012;8:823–9.
51. Liu L, Gardecki JA, Nadkarni SK, Toussaint JD, Yagi Y, Bouma BE, et al. Imaging the subcellular structure of human coronary atherosclerosis using micro-optical coherence tomography. Nat Med. 2011;17(8):1010–4.
52. Yoo H, Kim JW, Shishkov M, Namati E, Morse T, Shubochkin R, et al. Intra-arterial catheter for simultaneous microstructural and molecular imaging in vivo. Nat Med. 2011;17(12):1680–4.